ESAIM: M2AN
Vol. 41, N° 5, 2007, pp. 925–943
DOI: 10.1051/m2an:2007040

ESAIM: Mathematical Modelling and Numerical Analysis
www.esaim-m2an.org

THE SINGULARITY EXPANSION METHOD APPLIED TO THE TRANSIENT MOTIONS OF A FLOATING ELASTIC PLATE

Christophe Hazard[1] and François Loret[2]

Abstract. In this paper we propose an original approach for the simulation of the time-dependent response of a floating elastic plate using the so-called *Singularity Expansion Method*. This method consists in computing an asymptotic behaviour for large time obtained by means of the Laplace transform by using the analytic continuation of the resolvent of the problem. This leads to represent the solution as the sum of a discrete superposition of exponentially damped oscillating motions associated to the poles of the analytic continuation called resonances of the system, and a low frequency component associated to a branch point at frequency zero. We present the mathematical analysis of this method for the two-dimensional sea-keeping problem of a thin elastic plate (ice floe, floating runway, ...) and provide some numerical results to illustrate and discuss its efficiency.

Mathematics Subject Classification. 44A10, 35B34, 47A56, 11S23, 76B15.

Received November 19, 2006. Revised May 22, 2007.

1. Introduction

The main motivation of the present paper is the investigation of a numerical process which is able to provide quickly a reliable prediction of the transient response of a water wave problem.

The common techniques used for simulating propagation of transient waves are admittedly precise but too much time-consuming, from a numerical point of view: integral equations, Laplace transform, modal decompositions, finite difference schemes in time with absorbing boundary conditions or Perfectly Matched Layers, ... For this reason we consider an alternative to those techniques.

Considering the transient scattered wave, we can use the Prony's algorithm. In a classical paper [35], Prony proposed a method for interpolating a time-dependent solution by complex exponentials through a series of data values at equally spaced points. The methodology consists in solving a system of linear equations for the coefficients of a difference equation satisfied by the exponential functions, and obtained the exponential functions from the roots of the polynomial with those coefficients. This technique has been successfully applied to acoustics [29], electromagnetism [36] and even for black hole [5]. But this approach is useful only when the response can be modeled by a sum of complex exponentials and we will see in the sequel that this is not the case for our system. Moreover, the Prony's algorithm is well-known to perform poorly when the signal is embedded in noise, which imposes a drastic constraint on the numerical precision of the computation.

Keywords and phrases. Laplace transform, resonance, meromorphic family of operators, integral representation.

[1] Laboratoire POEMS, UMR 2706 CNRS/ENSTRA/INRIA, École Nationale Supérieure de Techniques Avancées, 32 boulevard Victor, 75739 Paris Cedex 15, France. Christophe.Hazard@ensta.fr

[2] Glaizer Group, Agence en Innovation, 15 bis rue Jean Jaurès, 92260 Fontenay-aux-Roses, France. Francois.Loret@glaizer.com

Another approach is to consider the scattered wave from a frequency point of view. We consider a technique based on the notion of resonances which appears in many branches of mathematics, physics and chemistry: the so-called *Singularity Expansion Method* (SEM). The SEM does not provide directly the time-dependent solution of the scattering problem but its asymptotic behaviour for large time. This method is based on the analytic properties of the response as a function of the complex frequency s associated to its Laplace transform (in time). The transient causal response actually appears as a path integral of the frequency response, where the path is contained in the causal Laplace half-plane $\Re e(s) > 0$. If the frequency response is continued analytically into the anti-causal half-plane $\Re e(s) < 0$, some singularities may appear. Then by deforming the path integral around those singularities, an approximation of the time dependent solution is determined. The singularities are of two kinds for our sea-keeping problem: poles of the analytic continuation, called resonances, and a branch point at $s = 0$ linked to the logarithmic singularity of the Green's function of the problem. The SEM consists then in considering the sum of a discrete superposition of exponentially damped oscillating modes, corresponding to residues associated to resonances, and an integral component associated to the integration along the branch cut $(\mathbb{R}^-)$ originating from $s = 0$. The error made with the SEM-approximation is exponentially decreasing in time.

Methods of analytic continuation have been extensively studied during the last 20 years as well from a mathematical analysis viewpoint as a numerical viewpoint. The different techniques can be collected in three families: integral representation [3, 24, 26, 34] (using a Green's function), series expansion [17] (by separation of variables) and analyticity dilation [2, 6] (complex scaling). The two first approaches reduce the extraction of resonances to the solution of a non linear eigenvalue problem and the third approach, to a linear one. In the present paper the analytic continuation following is performed by using an integral representation coupled with a variational approach and the resonances are extracted by searching the roots of matrix determinant.

The SEM approach was emphasized early from a theoretical point of view by Lax and Phillips [25] in 1969 for the scalar wave equation outside a bounded obstacle. They used their celebrated semi-group, which provides a connection between the stationary and the time-dependent states, and proved an expansion of the scattered waves for large time in odd dimensions and for non-trapping obstacles. Vainberg [42] obtained later the same results but with more direct arguments. Recently Burq, Tang and Zworski [9, 39] generalized the initial works by Lax and Phillips to even dimensions and trapping obstacles. Far from those theoretical works the SEM was originally devised from a numerical point of view by Baum [7] in the 70's to locate and discriminate objects by means of electromagnetic waves. Since the 1970's the SEM gave rise to many works essentially from a numerical point of view. The different works are mostly concerned with scalar electromagnetic and acoustic wave fields [15, 24, 31, 33, 40]. Even a physical interpretation of the SEM has been mentioned in term of creeping waves in [41]. In hydrodynamics the first application of the SEM was proposed in 1970 by Maskell and Ursell [30] for the sea-keeping of a half-immersed horizontal circular cylinder. They showed numerically that the vertical displacement appears as the sum of a damped harmonic motion, corresponding to a single pole, and a very small motion. Their approach does not yield any information about the fluid motion. We shall see here how the resonant modes provide this information. More recently Meylan [32] used the SEM to derive the solution of time-dependent motions of thin plate on shallow water (1D model). In this situation, no low-frequency motion occurs and a very good agreement between the transient motions and its polar approximation is observed. Also worth mentioning are the works by Schafer and Kouyoumjian [37] and, Felsen and Heyman [14]. Schafer and Kouyoumjian developed a functional interpolation between large (SEM approach) and short (high frequency asymptotic expansion or series decomposition) time-asymptotic solutions to determine the response for all time. Felsen and Heyman proposed with the same aim a hybrid method coupling the SEM and optical geometric tools respectively for low and high frequencies propagation phenomena.

The present paper is devoted to the mathematical analysis and the numerical study of the SEM applied to the two-dimensional sea-keeping problem of a thin elastic plate. This problem can model an ice floe or a floating runway. The paper is organized as follows. We start in Section 2 by introducing the linearized equations describing the small motions of our scattering problem and a general description of the principle of the SEM. In Section 3 we describe the mathematical analysis which leads to the proper functional framework for the application of the SEM and guides our numerical approach. Further details may be found in Loret [28]

including a mathematical analysis in the three-dimensional case. Finally in Section 4 we deal with the tools for the numerical implementation and provide some numerical results.

2. The 2D sea-keeping problem and the principle of the SEM

2.1. The 2D sea-keeping problem

We consider the two-dimensional motions of a thin elastic plate floating at the free surface of an inviscid perfect fluid whose motion is assumed irrotational. We denote $\Omega := \{(x,y) \in \mathbb{R}^2\,;\, y < 0\}$ the half-space filled by the water at rest. Its boundary $\partial\Omega := \{(x,y) \in \mathbb{R}^2\,;\, y = 0\}$ consists in two subdomains: P the domain filled by the plate and F the (fluid) free surface. Let the constants β and γ denote respectively flexibility and mass per unit length of the plate.

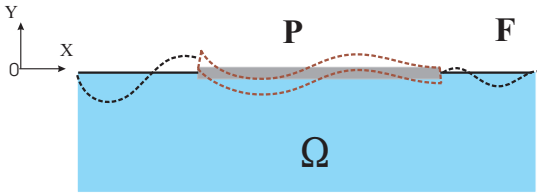

We present here a non-dimensional expression of the linearized equations which model the small motions of our system. It involves the acceleration potential Φ (in fact its opposite) and η which denotes as well the vertical displacement of the free surface as the one of the plate. We choose the acceleration potential instead of the usual velocity potential (the former is the time-derivative of the latter) so that our formulation involves only second order time-derivative. In the fluid domain we use the standard hydrodynamic equations (see *e.g.* [43]). The motion of the plate is described by the Kirchhoff-Love's model (see [11]). The time-dependent linearized sea-keeping problem consists in finding a pair $(\eta\,,\Phi)$ solution at every time $t > 0$ to the following coupled equations:

$$\Delta\Phi = 0 \quad \text{in } \Omega, \tag{1a}$$
$$\partial_t^2\eta + \partial_y\Phi = 0 \quad \text{on } \partial\Omega, \tag{1b}$$
$$-\Phi + \eta = 0 \quad \text{on } F, \tag{1c}$$
$$-\Phi + \eta + \beta\partial_x^4\eta - \gamma\partial_y\Phi = 0 \quad \text{on } P, \tag{1d}$$
$$\partial_x^2\eta = 0 = \partial_x^3\eta \quad \text{on } \partial P, \tag{1e}$$

as well as suitable initial conditions

$$\eta(0) = \eta_0 \quad \text{and} \quad \partial_t\eta(0) = \eta_1 \quad \text{on } \partial\Omega\,.$$

2.2. The principle of the SEM

We give in the sequel a general but formal presentation of the SEM following [16]. To this aim consider an abstract problem which consists in finding $u(t)$, a causal ($u(t) = 0\ \forall t < 0$) distribution of time with values in a complex Hilbert space $\mathcal{H}$, such that[1]

$$\mathrm{d}_t^2 u + \mathcal{A}u = f \quad \forall t \in \mathbb{R}. \tag{2}$$

The right hand side f of (2) takes into account the initial conditions as follows

$$f(t) := u(0) \otimes \mathrm{d}_t\delta(t) + \mathrm{d}_t u(0) \otimes \delta(t)$$

[1]Our sea-keeping problem enters this abstract framework (see [28]).

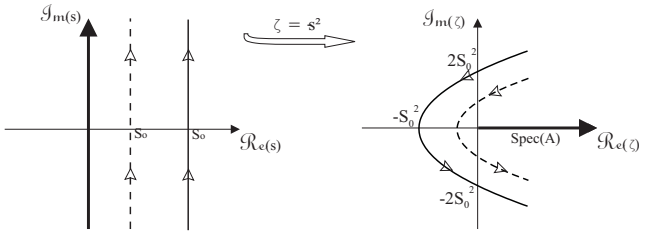

FIGURE 1. Displacement of the integration path.

where δ denotes the Dirac measure at $t = 0$. The operator $\mathcal{A}$ is assumed positive and self-adjoint in $\mathcal{H}$.

Consider the Laplace transform of $u(t)$ (which makes the link between the time domain and the frequency domain) formally[2] defined by

$$u(t) \mapsto \hat{u}(s) = \mathscr{L}(u) := \int_0^{+\infty} \mathrm{e}^{-st}\, u(t)\, \mathrm{d}t, \quad \text{with } s \in \mathbb{C} \text{ such that } \Re e(s) > 0.$$

Applying the Laplace transform to (2), which amounts to diagonalizing the time-derivative operator[3], yields

$$(s^2 + \mathcal{A})\, \hat{u}(s) = \hat{f}(s) \Longleftrightarrow \hat{u}(s) = \mathcal{R}(-s^2)\hat{f}(s).$$

The operator $\mathcal{R}(\zeta) := (\mathcal{A} - \zeta)^{-1}$, called the resolvent of $\mathcal{A}$, is defined everywhere in the complex ζ-plane except on the spectrum of $\mathcal{A}$ (contained in $\mathbb{R}^+$). As a consequence, $\mathcal{R}(-s^2)$ is well defined since $-s^2 \notin \mathbb{R}^+$ ($\Re e(s) > 0$). The inverse Laplace transform allows then to obtain the transient solution as follows:

$$u(t) = \mathscr{L}^{-1}(\hat{u}) := \frac{1}{2\mathrm{i}\pi} \int_{s_o + \mathrm{i}\mathbb{R}} \mathrm{e}^{st}\, \mathcal{R}(-s^2)\hat{f}(s)\, \mathrm{d}s, \quad \text{with } s_o > 0 \tag{3}$$

(in all generality s_o is such that the contour integration is to the right-hand side of any singularities of $\hat{u}$). The independence of this last expression with respect to $s_o > 0$ is a consequence of the analyticity of the resolvent with respect to $\zeta = -s^2$ in $\mathbb{C} \setminus \mathbb{R}^+$.

What happens to the expression (3) when the integration path $s_o + \mathrm{i}\mathbb{R}$ moves from the causal half plane $\Re e(s) > 0$, in which the resolvent $\mathcal{R}(-s^2)$ is analytic, toward the anti-causal half-plane $\Re e(s) < 0$? The response is a new way to numerically evaluate (3) called SEM. This approach, moving to anti-causal half-plane, is potentially numerically interesting because it can lead to a good approximation of the *continuous representation* (3) of u with a *discrete superposition* of exponentially damped oscillating modes: this is the main object of the paper. Figure 1 shows that the displacement of the integration path produces in the spectral ζ-plane a succession of parabolas which pinch progressively the spectrum $\mathrm{Spec}(\mathcal{A})$ of $\mathcal{A}$. And equation (3) tells us that the SEM requires to exhibit the analytic continuation of $\mathcal{R}(\zeta)\hat{f}(s)$ through the spectrum of $\mathcal{A}$. Since $\hat{f}(s) := s\, u(0) + \mathrm{d}_t u(0)$ is an entire function then only the analytic continuation $\mathcal{R}(\zeta)$ is needed.

Assume the resolvent extends in the whole complex s-plane except near isolated singularities which can be of two kinds: poles of the extension, called *resonances*, and branch points. By virtue of the self-adjointness of $\mathcal{A}$ the distribution of the singularities in the complex s-plane is symmetric with respect to the real s-axis.

Applying the residue theorem to expression (3) and assuming a vanishing contribution from the closing contour of the deformation path at infinity ($|s| = \infty$) yields (see [40] for an alternative approach taking into

[2]A rigorous definition of the Laplace transform requires to introduce the notion of vector-valued distributions with values in a Banach space. For the sake of clarity we do not call to mind this mathematical aspect (see Dautray-Lions [13]).

[3]The method which consists in diagonalizing the operator $\mathcal{A}$ in order to solve the transient problem (2) is the so-called *Generalized Eigenfunction Expansions*, see *e.g.* Hazard and Loret [18] as well as references therein.

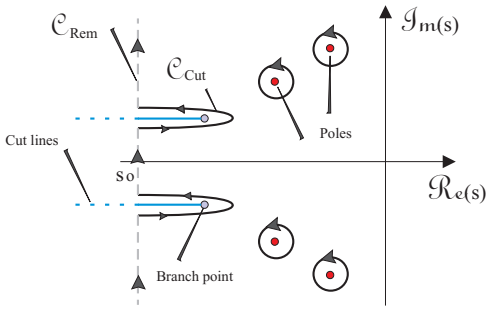

FIGURE 2. Deformation of the path.

account a non vanishing high frequency behavior)

$$u(t) = u_{\text{poles}}(t) + u_{\text{cut}}(t) + u_{\text{rem}}(t) \tag{4}$$

with

$$u_{\text{poles}}(t) := \sum_{\upsilon_k \in \{\xi \in \mathbb{C}\,;\, \Re e(\xi) > s_o\}} \frac{1}{2\mathrm{i}\pi} \int_{\circlearrowright_k} \mathrm{e}^{st}\, \mathcal{R}(-s^2) \hat{f}(s)\, \mathrm{d}s = \sum_k c_k(t)\, \mathrm{e}^{\upsilon_k t},$$

$$u_{\text{cut}}(t) := \frac{1}{2\mathrm{i}\pi} \int_{\mathscr{C}_{\text{Cut}}} \mathrm{e}^{st}\, \mathcal{R}(-s^2) \hat{f}(s)\, \mathrm{d}s,$$

$$u_{\text{rem}}(t) := \frac{1}{2\mathrm{i}\pi} \int_{\mathscr{C}_{\text{Rem}}} \mathrm{e}^{st}\, \mathcal{R}(-s^2) \hat{f}(s)\, \mathrm{d}s = O(\mathrm{e}^{s_o t}) \quad \text{as } t \to +\infty,$$

where $\int_{\circlearrowright_k}$ denotes the integration along a closed path enclosing a single pole υ_k and $c_k(t)\, \mathrm{e}^{\upsilon_k t}$ denotes the residue of $\mathrm{e}^{st}\, \mathcal{R}(-s^2) \hat{f}(s)$ associated to υ_k. Notice that when υ_k is a simple pole then c_k is constant in time. The polar component u_{poles} represents a discrete superposition of exponentially damped oscillating modes. The remainder term u_{rem} more decreasing than each element of u_{poles} is neglected by the SEM: the time-asymptotic behavior of $u(t)$ is obtained by considering only the polar component u_{poles} and the integral component u_{cut} in the decomposition (4).

The fact of "neglecting" the remainder term has no general theoretical base which could estimate the time required for doing that. In fact the question of time delay is central. Indeed, consider the acoustic wave propagation in the three-dimensional free space. It is well-known that the Green's function is an entire function of the Laplace variable. This induces that the analytic continuation of the resolvent has no singularity at all in that case and amounts to saying that $u(t) = u_{\text{rem}}(t)$. And for large time we know on the one hand from the Huygens' principle that locally in space $u_{\text{rem}}(t) = 0$ and on the other hand the SEM gives us $u(t) \simeq 0$. This example, which has no practical interest clearly, simply tells us that the SEM approximation is valid for large enough time and locally in space.

3. The resolvent and its analytic continuation

The first step for the application of the SEM consists in applying the Laplace transform in time to equations (1). Then we have to exhibit the analytic continuation of the resolvent of our problem, *i.e.* the operator which describes the resolution of equations (1) after application of the Laplace transform in time, to the left complex half-plane (anti-causal half-plane).

The analytic continuation is performed by using in Section 3.1 an integral representation of the Laplace transform of Φ. This approach analogous to that in [17] allows to reduce the Laplace transform of (1) to

a variational Fredholm equation defined on the plate domain. From a theoretical point of view, Steinberg's theorem [38] will provide in Section 3.3 the analytic continuation from this formulation by means of that of the Green's function of the free problem (that is the same problem without the plate). This formulation is also well adapted for a numerical computation of the resolvent and its singularities.

3.1. **The reduced problem**

As mention above, consider the Laplace transform of equations (1):

$$\Delta\hat{\Phi} = 0 \quad \text{in } \Omega, \tag{5a}$$

$$\partial_y\hat{\Phi} + s^2\hat{\eta} = s\eta_0 + \eta_1 =: \hat{f} \quad \text{on } \partial\Omega, \tag{5b}$$

$$-\hat{\Phi} + \hat{\eta} = 0 \quad \text{on } F, \tag{5c}$$

$$-\hat{\Phi} + \hat{\eta} + \beta\partial_x^4\hat{\eta} - \gamma\partial_y\hat{\Phi} = 0 \quad \text{on } P, \tag{5d}$$

$$\partial_x^2\hat{\eta} = 0 = \partial_x^3\hat{\eta} \quad \text{on } \partial P. \tag{5e}$$

From now on we omit the symbol $\hat{}$ without ambiguity. We use the well-known Green's function of the free problem (see [23,43]) to obtain an (implicit) integral representation of the acceleration potential Φ. We denote this Green's function $G_s(X, X')$ where $X = (x, y)$ and $X' = (x', y') \in \Omega$, $s \in \mathbb{C}$ such that $\Re e(s) > 0$ and

$$\left| \begin{array}{l} \Delta_X G_s(X, X') = \delta(X - X') \ \ \forall X \in \Omega, \\ \partial_y G_s(X, X') + s^2\, G_s(X, X') = 0 \ \ \forall X \in \partial\Omega. \end{array} \right.$$

This function is given by

$$G_s(X, X') = \mathrm{i}\,\mathrm{e}^{-s^2 w} + \frac{1}{2\pi}\left[\ln\left|\frac{z - \overline{z'}}{z - z'}\right| + \mathrm{e}^{-s^2 w}\, E_1(-s^2 w) + \mathrm{e}^{-s^2\overline{w}}\, E_1(-s^2\overline{w})\right]$$

where $z := x + \mathrm{i}y$, $z' := x' + \mathrm{i}y'$, $w := y + y' + \mathrm{i}|x - x'|$ and E_1 denotes the exponential integral function (see [1]). Note that when a function φ satisfies the following problem

$$\left| \begin{array}{l} \Delta\varphi = 0 \quad \text{in } \Omega, \\ \partial_y\varphi + s^2\varphi = h \quad \text{on } \partial\Omega, \end{array} \right. \tag{6}$$

where the given function h is assumed to have a compact support in $\partial\Omega$, then φ admits an integral representation given by

$$\varphi(X') \quad = \quad \int_{X\in\partial\Omega} G_s(X, X')\, h(X)\, \mathrm{d}X, \ \forall X' \in \Omega.$$

Let us define from now on the following notation: let Γ be a subset of $\mathbb{R}^2$, then $\overset{\Gamma}{*}$ denotes the convolution product on Γ. This allows to rewrite φ such as that

$$\varphi(X') \quad = \quad G_s \overset{\partial\Omega}{*} h(X'), \ \forall X' \in \Omega.$$

Now using equations (5a) and (5b) together with the Green's function we obtain:

$$\Phi = s^2 G_s \overset{\partial\Omega}{*} (\Phi_{|\partial\Omega} - \eta) + G_s \overset{\partial\Omega}{*} f(s) \quad \text{in } \Omega. \tag{7}$$

The integral representation (7) together with (5c) show that Φ is completely determined in Ω from the knowledge of $\psi := \Phi_{|P} - \eta_{|P}$ which satisfies

$$\psi = s^2 G_s \overset{P}{*} \psi + G_s \overset{\partial\Omega}{*} f(s) - \eta \quad \text{on } P. \tag{8}$$

Finally we obtain that solving equations (5) amounts to solving the following coupled problem defined on the bounded domain P and which comes from (8) and (5d):

$$\eta + \psi - s^2\, G_s \overset{P}{*} \psi = G_s \overset{\partial\Omega}{*} f \quad \text{on } P, \tag{9a}$$

$$\beta \partial_x^4 \eta - \psi + \gamma s^2 \eta = \gamma f \quad \text{on } P \tag{9b}$$

together with the limit conditions (5e).

The aim of what follows will be to exhibit the proper functional framework in which the problems (5) and (9)-(5e) are well-posed and equivalent.

3.2. **Functional framework**

Let us first remark that $\eta_{|F}$ is determined by (5c) as soon as the potential Φ is known. For this reason we discard $\eta_{|F}$ from the set of unknowns and we denote the restriction $\eta_{|P}$ simply by η in the sequel.

Theorem 3.1. *Let $f \in L^2(\partial\Omega)$ a compactly supported given function. Then problem the* (5) *is well-posed in $H^2(P) \times W(\Omega, F)$ assuming $\Re e(s) > 0$, with*

$$W(\Omega, F) := \left\{ \Psi \,;\, \tau\, \Psi \in L^2(\Omega),\ \Psi_{|F} \in L^2(F) \ \text{ and } \ \nabla\Psi \in (L^2(\Omega))^2 \right\},$$
$$\tau(X) := (1 + \|X\|^2)^{-1/2} \big(\ln(2 + \|X\|^2) \big)^{-1}.$$

Proof. Put $\eta = \lambda\tilde{\eta}$ where $\lambda \in \mathbb{C}\backslash\{0\}$ will be precised in the sequel. Consider the following variational formulation of equations (5)

$$\left| \begin{array}{l} \text{Find } \boldsymbol{u} = (\tilde{\eta}\,, \Phi) \text{ such that for all } v.g. = (\mu\,, \Psi) \\ \qquad a(\boldsymbol{u}\,, v.g.) = \dfrac{1}{\lambda\, s^2} \displaystyle\int_{\partial\Omega} f\, \overline{\Psi} - \gamma \int_P f\, \overline{\mu} \end{array} \right. \tag{10}$$

where

$$\begin{aligned} a(\boldsymbol{u}, v.g.) \ := \ & \frac{1}{\lambda\, s^2} \left(\int_\Omega \nabla\Phi \,.\, \nabla\overline{\Psi} + s^2 \left[\int_F \Phi\, \overline{\Psi} + \lambda \int_P \tilde{\eta}\, \overline{\Psi} \right] \right) \\ & - \left(\beta\, \lambda \int_P \partial_x^2 \tilde{\eta}\, \partial_x^2 \overline{\mu} + (1 + \gamma s^2)\, \lambda \int_P \tilde{\eta}\, \overline{\mu} - \int_P \Phi\, \overline{\mu} \right). \end{aligned}$$

We are going to establish the coercivity of the sesquilinear form $a(\cdot\,,\cdot)$ in the Hilbert space $H^2(P) \times W(\Omega, F)$.

$$\begin{aligned} \Im m\left(a(\boldsymbol{u}\,, \boldsymbol{u})\right) \ = \ & -\Im m(\lambda s^2) \left[\gamma \|\tilde{\eta}\|_P^2 + \frac{1}{|\lambda s^2|^2} \|\nabla\Phi\|_\Omega^2 \right] \\ & -\Im m(\lambda) \left[\beta \|\partial_x^2 \tilde{\eta}\|_P^2 + \|\tilde{\eta}\|_P^2 + \frac{1}{|\lambda|^2} \|\Phi\|_F^2 \right] \end{aligned}$$

where $\|\cdot\|_{\mathscr{O}}$ denotes the norm in $L^2(\mathscr{O})$. Put $\lambda = \exp(\mathrm{i}\theta)$ with $\theta \in \,]0, \pi - \arg(s^2)[$ when $\Im m(s) \geq 0$ and $\theta \in \,]-\pi - \arg(s^2), 0[$ when $\Im m(s) < 0$ (which has a sense since $|\arg(s^2)| \neq \pi$), then $\Im m(\lambda)$ and $\Im m(\lambda s^2)$ have the same sign. As a consequence

$$|a(\boldsymbol{u}, \boldsymbol{u})| \geq m \left[\|\nabla\Phi\|_\Omega^2 + \|\Phi\|_F^2 + \|\tilde{\eta}\|_P^2 + \|\partial_x^2 \tilde{\eta}\|_P^2 \right]$$
$$\text{where } \ m = \min\left\{ |\Im m(\lambda s^2)|, |\Im m(\lambda)| \right\} \min\left\{ 1/|s|^4, \beta, 1 \right\}.$$

Now the convexity inequalities of the Hilbert space $H^2(P)$, see Dautray-Lions [12], and the work by Amrouche [4] show respectively that $\|\cdot\|_P^2 + \|\partial_x^2 \cdot\|_P^2$ and $\|\nabla\cdot\|_\Omega^2 + \|\cdot\|_F^2$ define a norm in $H^2(P)$ and $W(\Omega, F)$ respectively

equivalent to the graph norm. So $a(\cdot\,,\cdot)$ is coercive in $H^2(P)\times W(\Omega,F)$. The statement of the theorem follows from Lax-Milgram's theorem. □

Now we derive from equations (9)-(5e) of the reduced problem, the following variational formulation:

$$\left|\begin{array}{c}\text{Find } \boldsymbol{u}=(\eta,\psi) \text{ such that for all } v.g.=(\mu\,,\phi)\\ \displaystyle\int_P \left(\psi+\eta-s^2\,G_s\overset{P}{*}\psi\right)\overline{\phi}+\int_P\left(\gamma s^2\eta-\psi\right)\overline{\mu}+\beta\int_P\partial_x^2\eta\,\partial_x^2\overline{\mu}\\ =\displaystyle\int_P\left(G_s\overset{\partial\Omega}{*}f(s)\right)\overline{\phi}+\gamma\int_P f(s)\,\overline{\mu}.\end{array}\right. \tag{11}$$

Theorem 3.2. *Let f belong in $L^2(\partial\Omega)$ with compact support. Consider the pair $(\eta\,,\Phi)\in H^2(P)\times W(\Omega,F)$ solution to* (5)*. Then the pair $(\eta\,,\psi)$, with $\psi:=\Phi_{|P}-\eta$, is solution to* (11) *in $\boldsymbol{\mathcal{H}}:=H^2(P)\times L^2(P)$. Conversely a pair $(\eta\,,\psi)\in\boldsymbol{\mathcal{H}}$ solution to* (11) *extends to a solution $(\eta\,,\Phi)$ to* (5) *in $H^2(P)\times W(\Omega,F)$ where Φ is defined by*

$$\Phi:=s^2G_s\overset{P}{*}\psi+G_s\overset{\partial\Omega}{*}f. \tag{12}$$

Proof. The statement of the theorem is a direct consequence of Section 3.1 and the fact that for all $h\in L^2(\partial\Omega)$, the convolution product $G_s\overset{\partial\Omega}{*}h$ defines the variational solution to (6) in $W(\Omega,\partial\Omega)$. This result is deduced from the properties of the Green's function G_s, see Loret [28] for details. □

3.3. **Fredholm context and Steinberg's theorem**

We are going to show that the variational formulation (11) falls within the Fredholm alternative which is a good framework both from a mathematical point of view, to exhibit the analytic continuation and for a Galerkin discretization. We will deduce from Theorem 3.4 that the computation of poles of the analytic continuation reduces to the resolution of a nonlinear eigenvalue problem. An application of the results in [38] (embedded in a more general framework in the book by Kato [19]) will provide in Section 3.4 an explicit expression for the computation of residues.

Consider the following rewriting of (11) where we choose in $H^2(P)$, for convenience, the norm

$$\sqrt{\|\cdot\|_P^2+\beta\|\partial_x^2\cdot\|_P^2}$$

equivalent to the standard norm (*cf.* proof of Thm. 3.1)

$$\left|\begin{array}{l}\text{Find } \boldsymbol{u}=(\eta,\psi)\in\boldsymbol{\mathcal{H}} \text{ such that}\\ \quad(\mathcal{I}+\mathcal{K}(s))\boldsymbol{u}=\mathcal{L}(s,f)\end{array}\right. \tag{13}$$

with for all $v.g.=(\mu,\varphi)\in\boldsymbol{\mathcal{H}}$

$$\begin{array}{rcl}(\mathcal{K}(s)\boldsymbol{u},v.g.)_{\boldsymbol{\mathcal{H}}} & := & (\eta,\varphi)+((\gamma s^2-1)\eta-\psi,\mu)-s^2(G_s*\psi,\varphi),\\ (\mathcal{L}(s,f),v.g.)_{\boldsymbol{\mathcal{H}}} & := & (G_s*f,\varphi)+\gamma\,(f\,,\mu),\end{array} \tag{14}$$

where $(\cdot\,,\cdot)$ denotes the scalar product of the Hilbert space $L^2(P)$ and $(\cdot,\cdot)_{\boldsymbol{\mathcal{H}}}$ that of $\boldsymbol{\mathcal{H}}$.

Proposition 3.3. *The operator $\mathcal{K}(s)$ is compact on $\boldsymbol{\mathcal{H}}$.*

Proof. First of all we rewrite the operator $\mathcal{K}(s)$. Let $\mathcal{E}_1$ and $\mathcal{E}_2$ be two operators from $\boldsymbol{\mathcal{H}}$ to $L^2(P)$ defined by $\mathcal{E}_1 v.g.:=\mu$ and $\mathcal{E}_2 v.g.:=\varphi$ for all $v.g.=(\mu\,,\varphi)\in\boldsymbol{\mathcal{H}}$. Let $\mathcal{T}(s)$ be the integral operator from $L^2(P)$ to $L^2(P)$ defined by

$$\mathcal{T}(s)\varphi:=(G_s\overset{P}{*}\varphi)_{|P}.$$

The operator $\mathcal{K}(s)$ can be then written

$$\mathcal{K}(s) = \mathcal{E}_2^* \, \mathcal{E}_1 - s^2 \, \mathcal{E}_2^* \, \mathcal{T}(s) \, \mathcal{E}_2 + \mathcal{E}_1^* \left[(\gamma s^2 - 1) \mathcal{E}_1 - \mathcal{E}_2 \right].$$

Now from the theorem of Rellich-Kondrachov, the operator $\mathcal{E}_1$ is compact. Concerning the integral operator $\mathcal{T}(s)$, its kernel G_s is L^2-integrable on $P \times P$ since the Green's function can be rewritten as follows (see *e.g.* [28])

$$G_s((x,0),(x',0)) = -\frac{\cos(s^2|x-x'|)}{\pi} \ln(s^2|x-x'|) + E(s^2|x-x'|) \tag{15}$$

where E is an entire function. As a consequence $\mathcal{T}(s)$ is a Hilbert-Schmidt operator and so in particular a compact operator, see *e.g.* [8]. The statement of the proposition then follows. □

We now deal with the meromorphic continuation of the resolvent of our problem.

Theorem 3.4. *The operator $(\mathcal{I}+\mathcal{K}(s))^{-1}$ extends analytically to $\mathbb{C}\setminus\mathbb{R}^-$ except near isolated singularities which are on the one hand poles of the extension, with finite multiplicity, and on the other hand a branch point at $s = 0$.*

Proof. First of all note that the analyticity of $\mathcal{K}(s)$ with respect to s is equivalent to the analyticity of $(\mathcal{K}(s)\boldsymbol{u}, v.g.)_{\boldsymbol{\mathcal{H}}}$ for all $\boldsymbol{u}$ and *v.g.* in $\boldsymbol{\mathcal{H}}$, see *e.g.* [19]. Now from (14) and the expression (15) of the Green's function, $\mathcal{K}(s)$ is clearly analytic in $\mathbb{C} \setminus \mathbb{R}^-$ with a logarithmic singularity at $s = 0$ (or analytic on the Riemann surface associated to the logarithm).

Since $\mathcal{K}(s)$ is compact on $\boldsymbol{\mathcal{H}}$ from Proposition 3.3, Steinberg [38] gives us the following alternative:

(i) either $\mathcal{I} + \mathcal{K}(s)$ is not invertible for all $s \in \mathbb{C} \setminus \mathbb{R}^-$;
(ii) either $(\mathcal{I} + \mathcal{K}(s))^{-1}$ is meromorphic in $\mathbb{C} \setminus \mathbb{R}^-$ and its singularities correspond to values $s \in \mathbb{C} \setminus \mathbb{R}^-$ for which -1 is an eigenvalue of $\mathcal{K}(s)$.

Now from Theorem 3.2 our problem (13) falls within the case (ii), the statement of the theorem then follows. □

The poles of $(\mathcal{I} + \mathcal{K}(s))^{-1}$ (which appears for a denumerable set) are named resonances of our problem. Those complex numbers are the solutions to the following non linear eigenvalue problem:

$$\left| \begin{array}{c} \text{Find } \upsilon \in \mathbb{C} \setminus \mathbb{R}^-, \, \Re e(\upsilon) \leq 0, \text{ and } \boldsymbol{u} = (\eta\,, \psi) \in \boldsymbol{\mathcal{H}} \setminus \{0\} \text{ such that} \\ (\mathcal{I} + \mathcal{K}(\upsilon))\, \boldsymbol{u} = 0. \end{array} \right. \tag{16}$$

3.4. **Computation of residues**

We are now dealing with the calculation of the residue of the solution $\boldsymbol{u}(s) = (\mathcal{I}+\mathcal{K}(s))^{-1}\mathcal{L}(s)$ at a resonance υ of order 1, that is in a neighborhood of υ

$$(\mathcal{I} + \mathcal{K}(s))^{-1} = \sum_{n=-1}^{+\infty} B_n \, (s-\upsilon)^n \quad \text{where} \quad B_{-1} \neq 0.$$

To this aim, we search an explicit expression of the term $\boldsymbol{u}^{(-1)}$ of the Laurent expansion of $\boldsymbol{u}(s)$ in the vicinity of υ

$$\boldsymbol{u}(s) = \sum_{n=-1}^{+\infty} (s-\upsilon)^n \, \boldsymbol{u}^{(n)}.$$

Ansatz. Let us remark that no general result on the multiplicity of the eigenvalues of $\mathcal{K}(\upsilon)$ is known for the present. Nevertheless many results in the literature let's think that it is quite reasonable to assume a generic simplicity of the resonances [20]. For this reason we make the following ansatz which will be confirmed by the numerical computation of (18):

Assume the eigenvalue -1 of $\mathcal{K}(\upsilon)$ is simple.

Let $\boldsymbol{w}_r$ and $\boldsymbol{w}_l$ be two vectors (right and left eigenvectors) such that $\ker(\mathcal{I}+\mathcal{K}(\upsilon)) = \mathrm{Span}\{\boldsymbol{w}_r\}$, $\ker(\mathcal{I}+\mathcal{K}^*(\upsilon)) = \mathrm{Span}\{\boldsymbol{w}_l\}$ and $(\boldsymbol{w}_r\,,\boldsymbol{w}_l)_{\boldsymbol{\mathcal{H}}} = 1$. Then the eigenprojection $\mathcal{P}(\upsilon)$ associated to the eigenvalue -1 of $\mathcal{K}(\upsilon)$ writes

$$\mathcal{P}(\upsilon) v.g. = (v.g.\,,\boldsymbol{w}_l)_{\boldsymbol{\mathcal{H}}}\,\boldsymbol{w}_r.$$

Theorem 3.5. *Assume υ is a resonance and -1 is a simple eigenvalue of $\mathcal{K}(\upsilon)$. If $\mathcal{P}(\upsilon)\,\mathcal{K}^{(1)}\,\boldsymbol{w}_r \neq 0$[4], then the residue writes*

$$\boldsymbol{u}^{(-1)} = \frac{(\mathcal{L}(\upsilon),\boldsymbol{w}_l)_{\boldsymbol{\mathcal{H}}}}{(\mathcal{K}^{(1)}\boldsymbol{w}_r,\boldsymbol{w}_l)_{\boldsymbol{\mathcal{H}}}}\;\boldsymbol{w}_r \tag{17}$$

where the eigenvalue $\lambda(s)$ of $\mathcal{K}(s)$ writes for small $|s-\upsilon| \neq 0$

$$\lambda(s) = -1 + (s-\upsilon)\lambda^{(1)} + O(s-\upsilon) \quad \textit{with} \quad \lambda^{(1)} \neq 0 \quad \textit{and}$$
$$\mathcal{K}(s) = \sum_{n=0}^{+\infty} (s-\upsilon)^n\,\mathcal{K}^{(n)}.$$

Proof. This is a particular formulation of a result obtained by Steinberg [38] which states that

$$(\mathcal{I}+\mathcal{K}(s))^{-1} = \frac{\mathcal{P}(\upsilon)}{(s-\upsilon)\,\lambda^{(1)}} + \mathcal{U}(s)$$

where $\mathcal{U}(s)$ is analytic at υ,

$$\mathcal{U}(\upsilon) = (\mathcal{I}+\mathcal{K}(\upsilon))^{-1}\,(\mathcal{I}-\mathcal{P}(\upsilon)),$$

and $\lambda^{(1)} \neq 0$ is given by

$$\lambda^{(1)} = \mathrm{tr}[\mathcal{K}^{(1)}\,\mathcal{P}(\upsilon)] = (\mathcal{K}^{(1)}\boldsymbol{w}_r,\boldsymbol{w}_l)_{\boldsymbol{\mathcal{H}}}.$$

So we obtain finally, since $\mathcal{L}(s)$ is analytic, that the residue writes:

$$\boldsymbol{u}^{(-1)} = \frac{\mathcal{P}(\upsilon)\,\mathcal{L}(\upsilon)}{\lambda^{(1)}} = \frac{(\mathcal{L}(\upsilon)\,,\boldsymbol{w}_l)_{\boldsymbol{\mathcal{H}}}}{(\mathcal{K}^{(1)}\boldsymbol{w}_r\,,\boldsymbol{w}_l)_{\boldsymbol{\mathcal{H}}}}\;\boldsymbol{w}_r.$$ □

4. Numerical implementation

The numerical implementation is performed as follows. The computation of a numerical approximation of the resolvent is the first stage to be accomplished. This yields in particular the possibility to compute the response of our problem by using the inverse Laplace transform in the right complex half-plane (this will be a way to obtain a reference solution). The integration of the resolvent along a path in the left complex half-plane provides the integral component of the SEM. Then we use a method of determination of resonances which consists in combining Rouché's theorem (based on the Cauchy's integral, see Knopp [21]) and the iterative Newton-Raphson's method. Finally the computation of residues is drawn from Section 3.4.

[4]That is -1 is not a degenerate eigenvalue.

4.1. **Numerical approximation of the resolvent**

Consider first a subdivision $\{x_k\,,\,1\leq k\leq N\}$ of the plate $P:=[-1,+1]$ where $-1=:x_1<x_2<\ldots<x_{N-1}<x_N:=1$. The chosen scheme of discretization consists in coupling two techniques. A discretization by the Lagrange finite element basis $\{w_j\}$ of order 1 for ψ and a modal discretization of the vertical displacement η of the plate composed of free natural modes[5] w_μ of the plate, *i.e.* the eigenfunctions of $\beta\partial_x^4+\mathcal{I}$ satisfying the limit conditions (5e). Those modes are obtained analytically either as a rigid mode $ax+b$ with $(a,b)\in\mathbb{R}^2$, associated to the eigenvalue $\lambda_1=1$, or as a linear combination of $\cos(\alpha_\nu x)$, $\sin(\alpha_\nu x)$, $\cos\mathrm{h}(\alpha_\nu x)$ and $\sin\mathrm{h}(\alpha_\nu x)$. The coefficients α_ν represent the solutions to the dispersion equation $\tan(\alpha)=\pm\tan\mathrm{h}(\alpha)$. The associated eigenvalues write $\lambda_\nu=\beta\alpha_\nu^4+1$.

The discretization of the variational formulation (11) then yields the following matrix system:

$$(\mathbb{J}_h+\mathbb{K}_h(s))\begin{pmatrix}\boldsymbol{\eta}_h\\ \boldsymbol{\psi}_h\end{pmatrix}=\boldsymbol{L}_h(s)$$

with

$$\mathbb{J}_h:=\begin{bmatrix}\beta\left(\partial_x^2\mathrm{w}_\nu,\partial_x^2\mathrm{w}_\mu\right)+\left(\mathrm{w}_\nu,\mathrm{w}_\mu\right) & 0\\ 0 & \left(w_j\,,w_i\right)\end{bmatrix},$$

$$\boldsymbol{L}_h(s):=\begin{bmatrix}\gamma\left(w_j,\mathrm{w}_\mu\right) & 0\\ 0 & \left(G_s*w_j,w_i\right)\end{bmatrix}\begin{pmatrix}\boldsymbol{f}_h\\ \boldsymbol{f}_h\end{pmatrix},$$

$$\mathbb{K}_h(s):=\begin{bmatrix}(\gamma\,s^2-1)\left(\mathrm{w}_\nu,\mathrm{w}_\mu\right) & -\left(w_j,\mathrm{w}_\mu\right)\\ \left(\mathrm{w}_\nu,w_i\right) & -s^2\left(G_s*w_j,w_i\right)\end{bmatrix}.$$

The matrix $\mathbb{J}_h$ is obviously symmetric and positive definite. Exactly as in the continuous case the matrix $\mathbb{K}_h(s)$ and the vector $\boldsymbol{L}_h(s)$ are holomorphic and our discrete problem extends analytically in $\mathbb{C}\setminus\mathbb{R}^-$. The vector $\boldsymbol{\eta}_h$ denotes the coordinates of η in $\{\mathrm{w}_\mu\}$, and $\boldsymbol{\psi}_h$ and $\boldsymbol{f}_h$ those of ψ and f in $\{w_j\}$. All the terms of $\mathbb{J}_h$, $\mathbb{K}_h(s)$ and $\boldsymbol{L}_h(s)$ are obtained classically by using a numerical quadrature formula except those involving the Green's function: we used a Gauss-Legendre numerical integration formula. Indeed, the Green's function has a logarithmic singularity which requires a special treatment. In fact we have established an analytic formula for the extraction of the singularity of terms involving the kernel G_s, inspired from an original work by Marc Lenoir, see [28]. We can also mention that in the 3D case the same results are demonstrated with the same logarithmic behaviour of the Green's function, see Loret [28].

4.2. **Computation of resonances and resonant states**

The calculation of resonances is carried out in two steps by using the characterization (16).

We start with a first approximation of resonances (a initial guess) which insures we are missing none of them in a given region. The technique we use for that is based on Rouché's theorem and consists in looking for zeros of the determinant $\det(\mathbb{J}_h+\mathbb{K}_h(s))$ considered as an analytic function of the complex parameter s. Consider a closed contour $\mathscr{C}$ in the complex s-plane that does not intersect the negative s-axis. The theory of complex

[5]There are of course other possibilities to discretize the vertical displacement of the plate: for example the Hermite finite element. The main advantage of our choice is the possibility to extend easily our work to the 3D case.

variable tells us that

$$\frac{1}{2\mathrm{i}\pi}\int_{\mathscr{C}} s^k \frac{\det(\mathbb{J}_h+\mathbb{K}_h(s))}{\mathrm{d}_s\det(\mathbb{J}_h+\mathbb{K}_h(s))}\,\mathrm{d}s = \sum_{j=1}^{n} \upsilon_j^k =: \sigma_k \tag{18}$$

where υ_j, $j=1...n$, are all the zeros of $\det(\mathbb{J}_h+\mathbb{K}_h(s))$ which lie in the interior of $\mathscr{C}$ (a multiple zero is counted according to its multiplicity[6]). With $k=0$ we obtain the number of resonances in the given region. By Newton's identity (see [10]) one may construct a polynomial P_n which has the υ_j as roots from the knowledge of the σ_k, $k=1...n$.

Remark 4.1. In order to avoid the ill-conditioning of the determination of the roots of the polynomial P_n we subdivide if necessary the given region into smaller ones to consider a number n of resonances small enough[7].

The evaluation of the integral (18) requires the computation of the logarithmic derivative of $\det(\mathbb{J}_h+\mathbb{K}_h(s))$. We use here a technique based on an analytic differentiation of the LU-algorithm described in [24]. This technique allows to compute the logarithmic derivative of $\det(\mathbb{J}_h+\mathbb{K}_h(s))$ without computing neither $\det(\mathbb{J}_h+\mathbb{K}_h(s))$ nor its s-derivative from the knowledge of $\mathbb{J}_h+\mathbb{K}_h(s)$ and $\mathrm{d}_s\mathbb{K}_h(s)$. Note that $\mathrm{d}_s\mathbb{K}_h(s)$ is easily deduced (*cf.* equation (14)) from d_sG_s which is known analytically.

The second step refines the primary approximation of resonances, obtained in the first step, by solving the discretized version of the nonlinear eigenvalue problem (16):

$$\left|\begin{array}{l}\text{Find } \upsilon\in\mathbb{C}\setminus\mathbb{R}^-,\ \Re e(\upsilon)\le 0, \text{ and } \boldsymbol{u}_h=(\boldsymbol{\eta}_h\,,\boldsymbol{\psi}_h)^t\neq 0 \text{ such that}\\ \qquad\qquad (\mathbb{J}_h+\mathbb{K}_h(\upsilon))\boldsymbol{u}_h=0.\end{array}\right.$$

To solve this problem we use the iterative Newton-Raphson's method combined with the inverse power method. The Newton-Raphson's method consists in an approximation of the fixed points of $s-\mu_h(s)/\mathrm{d}_s\mu_h(s)$ where $\mu_h(s)$ is the smallest eigenvalue of $\mathbb{J}_h+\mathbb{K}_h(s)$. Using the previous computation of υ_j as initial guesses, this yields the resonances with a better precision. Assuming the eigenvalue $\mu_h(s)$ simple, the inverse power method provides an approximation of both $\mu_h(s)$ and its associated eigenvector. A resonant state is nothing else but the eigenvector associated to a resonance. It remains now to explain the computation of the s-derivative $\mathrm{d}_s\mu_h(s)$. Let us define $\boldsymbol{W}_r(s)$ and $\boldsymbol{W}_l(s)$ respectively the right and left eigenvectors by

$$\mathbb{K}_h(s)\,\boldsymbol{W}_r(s)=(\mu_h(s)-1)\,\mathbb{J}_h\,\boldsymbol{W}_r(s) \quad\text{and}\quad \boldsymbol{W}_l^*(s)\,\mathbb{K}_h(s)=(\mu_h(s)-1)\boldsymbol{W}_l^*(s)\,\mathbb{J}_h. \tag{20}$$

Then we deduce from (20) that

$$\mathrm{d}_s\mu_h(s)=\frac{\boldsymbol{W}_l^*(s)\,\mathrm{d}_s\,\mathbb{K}_h(s)\,\boldsymbol{W}_r(s)}{\boldsymbol{W}_l^*(s)\,\mathbb{J}_h\,\boldsymbol{W}_r(s)}.$$

[6]This will be a way to verify our assumption on the simplicity of the computed eigenvalues.

[7]We looked for other alternatives which do not require to subdivide the given region to limit the degree of the polynomial. Tien-Yen Li described in his paper [27] a stable method based on homotopy continuation to find all solutions to

$$\left|\begin{array}{l}\upsilon_1+\upsilon_2+\ldots+\upsilon_n=\sigma_1\\ \\ \upsilon_1^2+\upsilon_2^2+\ldots+\upsilon_n^2=\sigma_2\\ \vdots\\ \upsilon_1^n+\upsilon_2^n+\ldots+\upsilon_n^n=\sigma_n\end{array}\right. \tag{19}$$

without constructing the polynomial P_n. The method used reduces the resolution of (19) to the resolution of a ordinary differential equation. Another possibility developed by Kravanja and Van Barel [22] consists in computing separately the distinct zeros and their multiplicity. The first step makes a calculation of the zeros solving a generalized eigenvalue problem. Then the respective multiplicity are obtained simply in solving a Vandermonde system. Unfortunately those methods which are really interesting when we consider a path $\mathscr{C}$ enclosing several resonances, say more than 4, need an accurate calculation of the quantities σ_k and this computation in our case is highly time consuming.

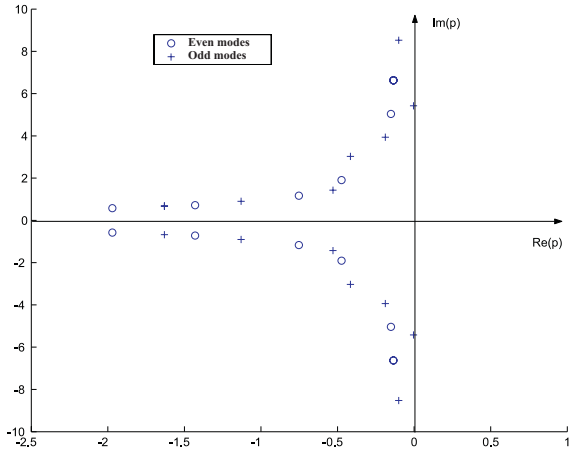

Real part	Imaginary part
−1.97013	± 0.57661
−1.63017	± 0.67725
−1.42960	± 0.71939
−1.12970	± 0.90598
−0.75226	± 1.17063
−0.52950	± 1.42717
−0.47359	± 1.90782
−0.41570	± 3.02755
−0.18777	± 3.93866
−0.15117	± 5.03931
−0.00361	± 5.42444
−0.13497	± 6.62686
−0.10006	± 8.52498

FIGURE 3. Distribution of numerical poles.

4.3. **Computation of residues**

We need here to Now for the computation of the residue of the solution of our matrix problem in the vicinity of a resonance υ_j, the result we have obtained in Section 3.4 can be directly applied here and yields

$$\begin{pmatrix} \boldsymbol{\eta}_h^{(-1)} \\ \\ \boldsymbol{\psi}_h^{(-1)} \end{pmatrix} = \frac{\boldsymbol{W}_l^*(\upsilon_j)\, \boldsymbol{L}_h(\upsilon_j)}{\boldsymbol{W}_l^*(\upsilon_j)\, \mathbb{K}_h^{(1)}\, \boldsymbol{W}_r(\upsilon_j)}\ \boldsymbol{W}_r(\upsilon_j)$$

where $\mathbb{K}_h(\upsilon_j)\, \boldsymbol{W}_r(\upsilon_j) = -\mathbb{J}_h\, \boldsymbol{W}_r(\upsilon_j)$, $\boldsymbol{W}_l^*(\upsilon_j)\, \mathbb{K}_h(\upsilon_j) = -\boldsymbol{W}_l^*(\upsilon_j)\, \mathbb{J}_h$ and such that $\boldsymbol{W}_l^*(\upsilon_j)\, \mathbb{J}_h\, \boldsymbol{W}_r(\upsilon_j) = 1$.

4.4. **Numerical experiments**

We report in this last subsection the outcome of a numerical application. It is a matter of a typical application for floating runways.

Set the constants β and γ respectively equal to 0.003 and 0.02. The plate (beam) coincide with the segment $[-1, +1]$. For the application we choose a very low and a low frequencies tests[8]. The very low frequency test consists in a null initial velocity, $\eta_1 = 0$, and a gaussian initial displacement of the surface, $\eta_0(x) = \exp(-3(x-2.5)^2)$. The low frequency test consists in a null initial velocity and for the initial displacement of the surface $\eta_0(x) = \cos(w_o x)\exp(-3(x-2.5)^2)$ with $w_o = 0.7$ (this is nearly the imaginary part of a resonance). The reader can wonder why higher frequency tests are not considered. The reason is simply that for the present, as shown in Figure 3, we are not able to compute, if any, sufficiently resonances with great imaginary part.

Preliminary. We first start with a presentation in Figure 3 of the distribution of numerical resonances in the complex plane followed by the representation of some resonant modes in Figures 4, 5 and 6. The cross (respectively circle) symbol in Figure 3 indicates a resonance associated to a anti-symmetric (respectively symmetric) mode. The dotted lines in Figures 4, 5 and 6 represent the acceleration potential and the continuous lines represent the displacement of the plate. Let us recall that outside the plate, displacement of the free surface and acceleration potential coincide.

The exploration of the complex plane for the computation of the first approximation of resonances by means of the technique based on the Cauchy's integral gave rise to numerical difficulties. Indeed, this approach provides

[8]These initial conditions are able to excite resonances which imaginary parts lie in the vicinity of 0 or $\pm\, w_o$. See Loret [28] for details and some other situations.

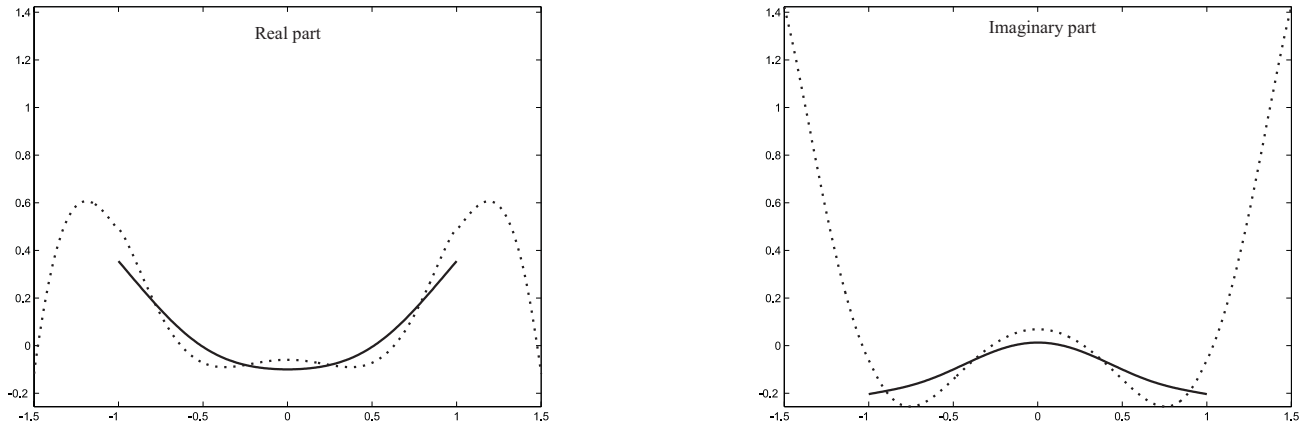

FIGURE 4. Resonant mode associated to $\upsilon_j = -1.97013 + \mathrm{i}\,0.57661$.

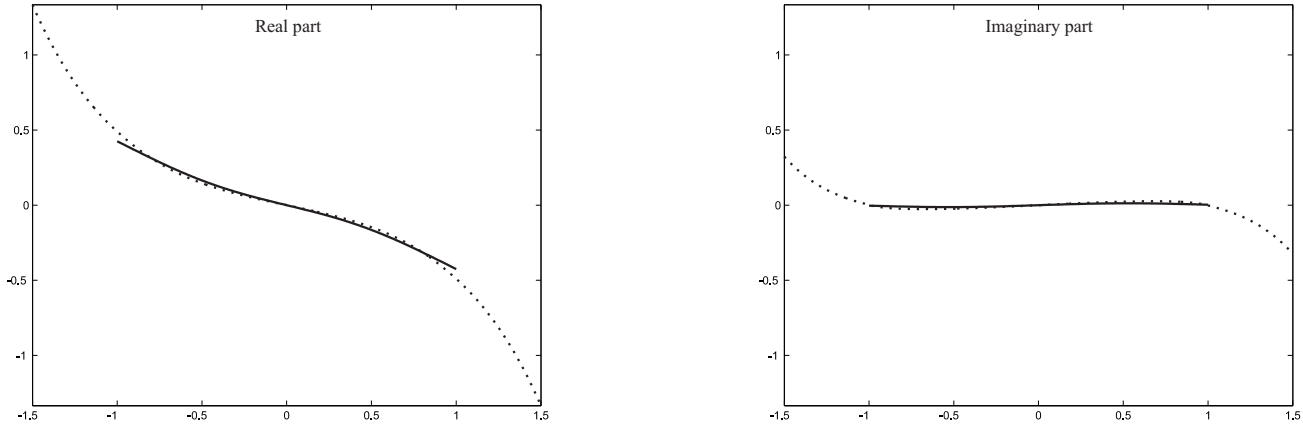

FIGURE 5. Resonant mode associated to $\upsilon_j = -1.12970 + \mathrm{i}\,0.90598$.

the starting trial value of the resonance and if it is not reasonably close to a real resonant pole then the iterative Newton-Raphson procedure may not lead to the exact pole position (because the pole search needs longer iteration with unusually larger number of steps). This limitation is difficult to quantify but this is probably due on the one hand to a constraint on the discretization in relation with the frequencies considered. On the other hand this fact is due to the terms related to the Green's function in the matrix system which becomes exponentially increasing when $\Im m(s) < 0$: this bad behaviour is a direct heritage of the exponentially increasing behaviour of the Green's function G_s when s belongs to the left complex half-plane.

The very low frequency test. In order to evaluate the efficiency of the *Singularity Expansion Method* we represent in Figure 7 the following relative error:

$$\mathrm{Err}(t) := \frac{\|\eta^h_{\mathrm{ref}}(t) - \eta^h_{\mathrm{poles}}(t) - \eta^h_{\mathrm{cut}}(t)\|_{P,h}}{\|\eta^h_{\mathrm{ref}}(t)\|_{P,h}}$$

where $\|v\|^2_{P,h} := \sum_\nu \lambda_\nu \left(v, \mathrm{w}_\nu\right)^2$ and λ_ν denotes the eigenvalue associated to w_ν. The components η^h_{poles} and η^h_{cut} denote respectively the numerical approximations of η_{poles} and η_{cut}. The component η^h_{ref} is a numerical

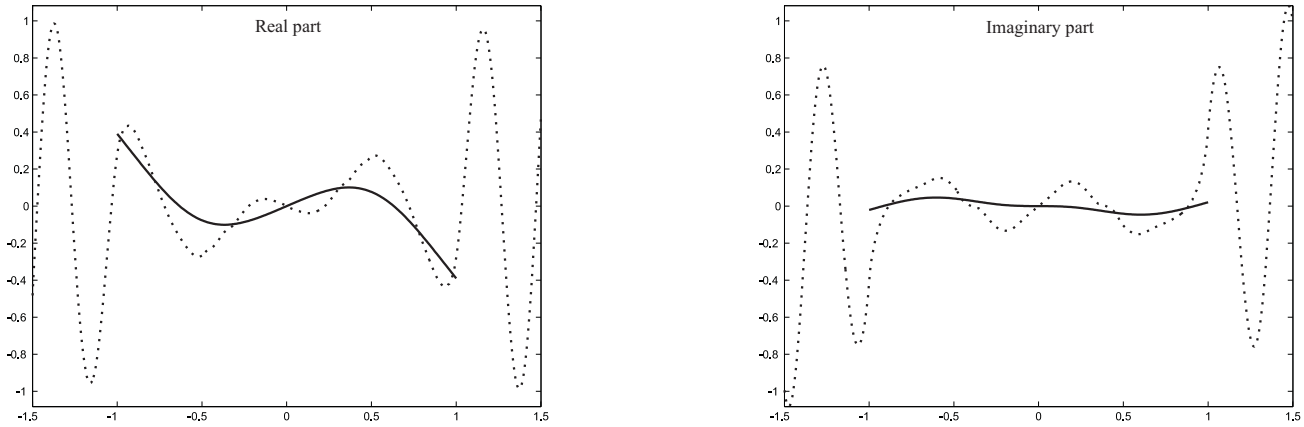

FIGURE 6. Resonant mode associated to $\upsilon_j = -0.18777 + \mathrm{i}\,3.93866$.

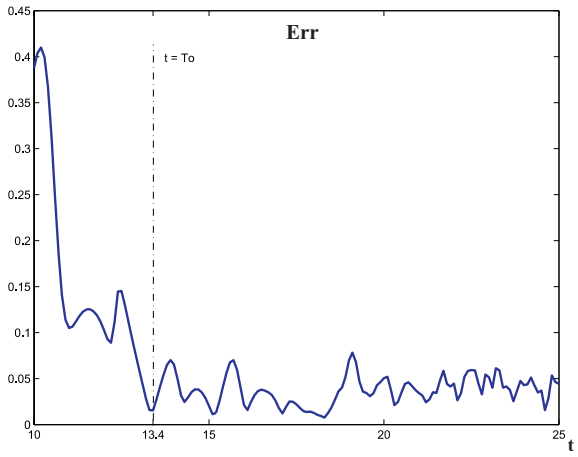

FIGURE 7. Relative error.

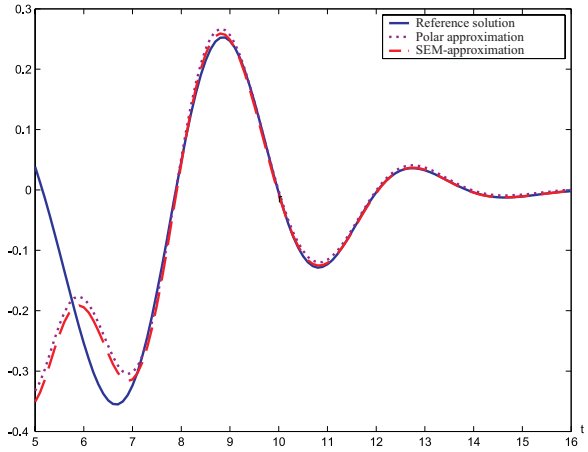

FIGURE 8. Solutions compared at the position $x_0 = -0.5$.

approximation of the solution obtained by means of the inverse Laplace transform integration, using formula (3) with $s_o = 0.2$, and is considered here as a reference solution.

Figure 7 shows around 4% error after the necessary time $T_o \simeq 13.4$ for the incident wavefront to pass over the plate entirely. This shows that the SEM is reliable once the incident wavefront has passed over the plate. This last numerical observation not only confirms that our approach catch the large time behaviour of the diffracted part of the waves, but also furnishes an estimation or an idea of what means "large time". The following Figures 9 and 10 tells us more again. Those figures represent in the same graphic the reference displacement $\eta^h_{\mathrm{ref}}(x_o, t)$ in solide line and its SEM-approximation $\eta^h_{\mathrm{poles}}(x_o, t) + \eta^h_{\mathrm{cut}}(x_o, t)$ in dotted line at $x_o = 0.5$ and $x_o = -0.5$. We can see that when the wavefront has passed over the observed position x_o, that is as soon as $t \simeq 7$ for $x_o = 0.5$ and $t \simeq 9.5$ for $x_o = -0.5$, the SEM provides a reasonable approximation of $\eta^h(x_o, t)$.

Also worth mentioning is the fact that about 95% of the signal can be recontructed by considering only two poles together with their conjugate in the SEM-approximation. This observation is close to earlier numerical

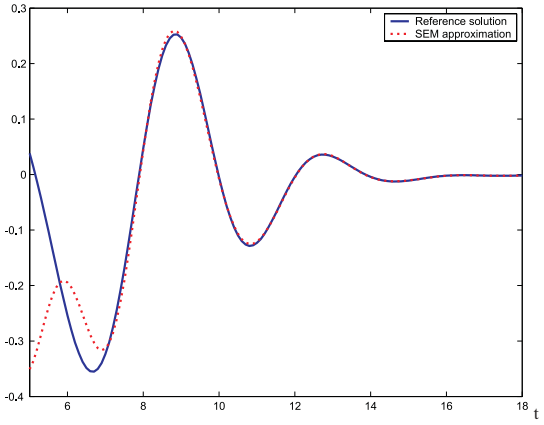

FIGURE 9. Comparison at $x_o = 0.5$.

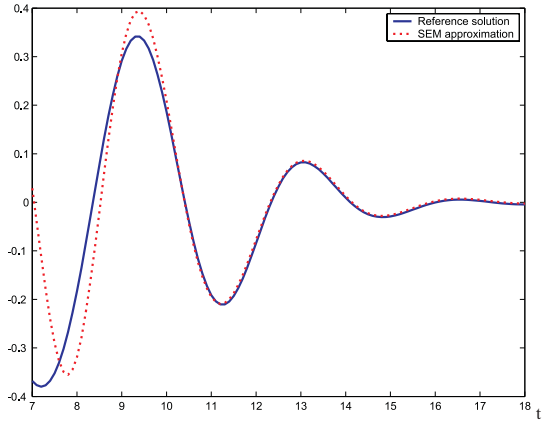

FIGURE 10. Comparison at $x_o = -0.5$.

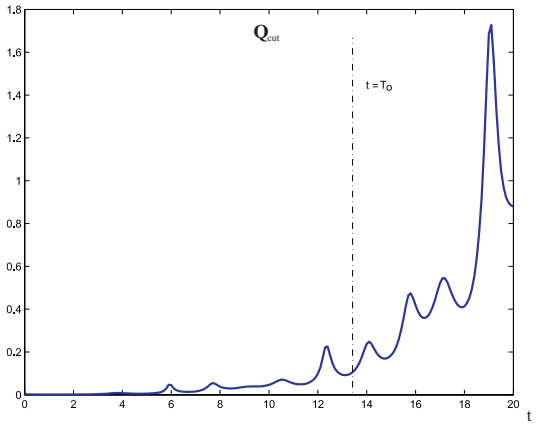

FIGURE 11. Cut line influence.

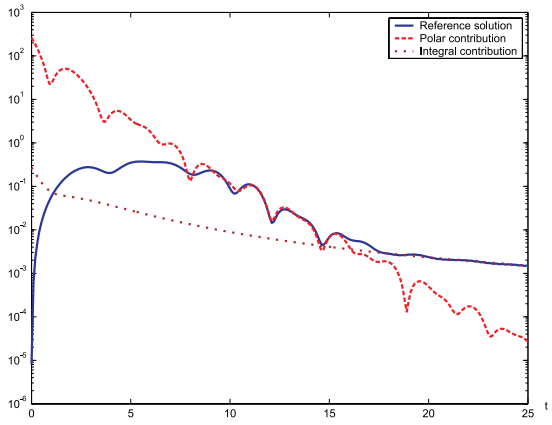

FIGURE 12. Log contribution representation.

experiment of Maskell and Ursell [30] for the sea-keeping of a half-immersed horizontal circular cylinder where only one pole was required to simulate one degree of freedom.

Since the component η^h_{cut} is the one which requires a costly calculation, indeed this term depends on the excitation, we decide to evaluate its proportion in the SEM-approximation *via*

$$\mathrm{Q}_{\text{cut}}(t) := \frac{\|\eta^h_{\text{cut}}(t)\|_{P,h}}{\|\eta^h_{\text{poles}} + \eta^h_{\text{cut}}(t)\|_{P,h}}.$$

Figure 11 shows that the part of the integral component grows with the time which is not a surprise since the polar component is exponentially decreasing. But the relatively importance of the integral component must be moderated since Figure 12 which represents $\log(\|\eta^h_{\text{ref}}(t)\|_{P,h})$ in solid line, $\log(\|\eta^h_{\text{pole}}(t)\|_{P,h})$ in discontinuous line and $\log(\|\eta^h_{\text{cut}}(t)\|_{P,h})$ in dotted line, shows that not only the integral component is non oscillating and slowly decreasing but above all is relatively small. This last observation is illustrated by the following Figure 8 which represents at the position $x_0 = -0.5$ the reference solution in solid line, the SEM-approximation in discontinuous line and the polar component in dotted line. This figure indicates a difference less than 0.01

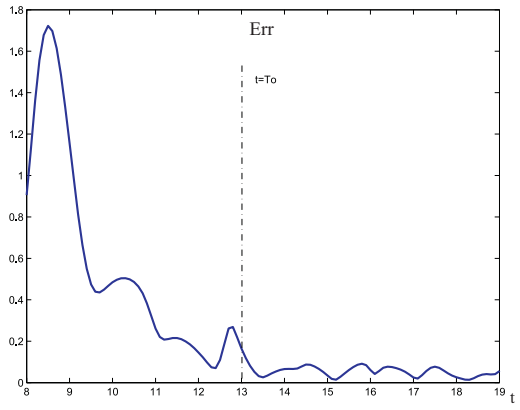

FIGURE 13. Relative error.

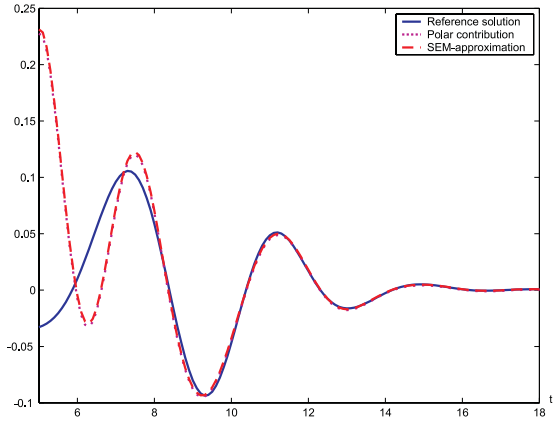

FIGURE 14. Solution compared at the position $x_o = 0.5$.

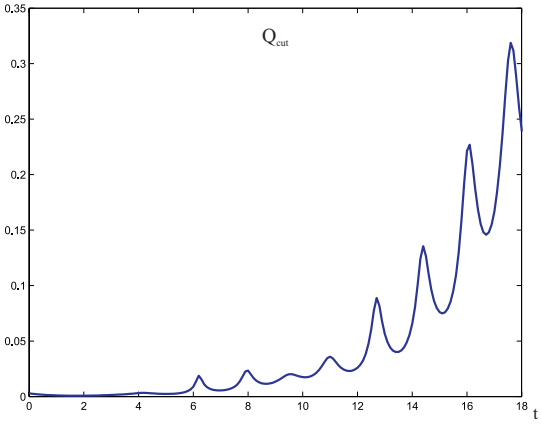

FIGURE 15. Cut line influence.

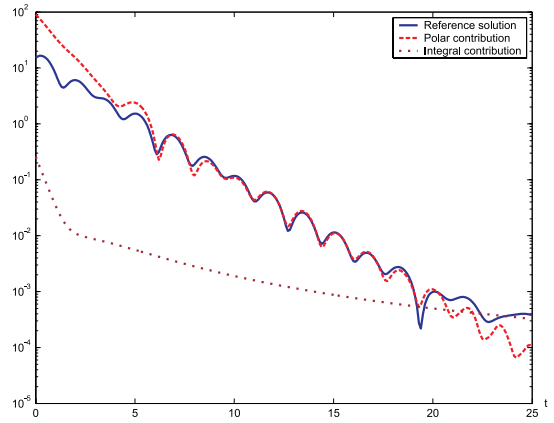

FIGURE 16. Log contribution representation.

between the amplitude of the SEM-approximation and the polar component once the incident wavefront has passed over the position x_0, that is around $t \simeq 7$.

Low frequency test. Notice that we choose here data capable to excite resonances whose imaginary part lies in the vicinity of $\pm w_o$. We get for this second numerical experiment globally the same observations as previously. Figure 13 shows the SEM provides an error between 2 and 7% error, from the time $T_o \simeq 13$. As previously very few resonances are required to construct the approximaton: three poles together with their conjugate are sufficient to construct more than 95% of the SEM-approximation. Figure 14 shows that around $t = 8$, that is once the incident wave front has passed over the observed position x_0, the part of the integral component is not significant.

The novelty of this test comes essentially from Figures 15 and 16. They show that not only this time the integral component η^h_{poles} is relatively smaller than in the previous test, compared to η^h_{cut}, but its amplitude is smaller too. The lack of computed resonances prevents us for the present from a real numerical study of this observation. For further works it is interesting to verify when we choose data that do not excite the frequency zero, but higher and higher frequencies, whether or not the integral component becomes smaller and smaller.

5. Conclusion

First of all it is important to mention for further works that the main advantage of the Singularity Expansion Method is that the resonances and associated resonant modes are independent of the excitation and can be computed just once and save, for a fixed material. And the approach we developed here can be extended to more realistic situations since our numerical tools extend easily to the three-dimensional case.

As pointed out earlier by Schafer and Kouyamjian [37] in 1975 but in an electromagnetism context, we show the capability of the SEM for re-building the time-dependent response once the incident wavefront has passed over the plate completely. This result shows that after this delay the remainder term can be considered negligible and the SEM becomes useful.

The numerical experiments which we undertook gave conclusions similar to those obtained by Maskell and Ursell [30] in 1970 for a simpler sea-keeping problem. Firstly we observed that a reasonable approximation can be obtained by retaining only few resonances in the polar component, two or three in our case. Secondly the integral component, which is associated to the cut line and requires a costly calculation for each excitation at each time t, has a slow decay but it appears with a small amplitude. In our experiments this component is so small that the polar component alone is enough to represent the SEM-approximation.

Another observation which requires again more investigation is the fact that the integral component has a smaller amplitude in the low frequency test than in the very low frequency one, when the given data do not excite "preferentially" a vicinity of the null frequency. And the question is: is the integral component becoming smaller and smaller when the data excite higher and higher frequencies?

References

[1] M. Abramowitz and I.A. Stegun, *Handbook of mathematical functions*. Dover Publications, New York, 9th edn. (1970).

[2] J. Aguilar and J.M. Combes, A class of analytic perturbations for one-body Schrödinger hamiltonians. *Comm. Math. Phys.* **22** (1971) 269–279.

[3] C. Alves and T. Ha Duong, Numerical experiments on the resonance poles associated to acoustic and elastic scattering by a plane crack, in *Mathematical and Numerical Aspects of Wave Propagation*, E. Bécache *et al.* Eds., SIAM (1995).

[4] C. Amrouche, The Neumann problem in the half-space. *C. R. Acad. Sci. Paris Ser. I* **335** (2002) 151–156.

[5] A. Bachelot and A. Motet-Bachelot, Les résonances d'un trou noir de Schwarzschild. *Ann. Henri. Poincarré* **59** (1993) 280–294.

[6] E. Balslev and J.M. Combes, Spectral properties of many body Schrödinger operators with dilation analytic interactions. *Comm. Math. Phys.* **22** (1971) 280–294.

[7] C.E. Baum, The Singularity Expansion Method, in *Transient Electromagnetic Fields*, L.B. Felsen Ed., Springer-Verlag, New York (1976).

[8] H. Brezis, *Analyse fonctionnelle, Théorie et application*. Masson, Paris (1983).

[9] N. Burq and M. Zworski, Resonance expansions in semi-classical propagation. *Comm. Math. Phys.* **232** (2001) 1–12.

[10] M.P. Carpentier and A.F. Dos Santos, Solution of equations involving analytic functions. *J. Comput. Phys.* **45** (1982) 210–220.

[11] P.G. Ciarlet and P. Destuynder, A justification of the two-dimensional linear plate model. *J. Mécanique* **18** (1979) 315–344.

[12] R. Dautray and J.L. Lions, *Analyse mathématique et calcul numérique pour les sciences et les techniques*. Tome 1, Dunod, Paris (1984).

[13] R. Dautray and J.L. Lions, *Analyse mathématique et calcul numérique pour les sciences et les techniques*. Tome 3, Dunod, Paris (1985).

[14] L.B. Felsen and E. Heyman, Hybrid ray mode analysis of transient scattering, in *Low and Frequency Asymptotics*, V.K. Varadan and V.V. Varadan Eds. (1986).

[15] D. Habault and P.J.T. Filippi, Light fluid approximation for sound radiation and diffraction by thin elastic plates. *J. Sound Vibration* **213** (1998) 333–374.

[16] C. Hazard, The Singularity Expansion Method, in *Fifth International Conference on Mathematical and Numerical Aspects of Wave propagation*, *SIAM* (2000) 494–498.

[17] C. Hazard and M. Lenoir, Determination of scattering frequencies for an elastic floating body. *SIAM J. Math. Anal.* **24** (1993) 1458–1514.

[18] C. Hazard and F. Loret, Generalized eigenfunction expansions for conservative scattering problems with an application to water waves. *Proceedings of the Royal Society of Edinburgh* (2007) Accepted.

[19] T. Kato, *Perturbation theory for linear operators*. Springer-Verlag, New York (1984).

[20] F. Klopp and M. Zworski, Generic simplicity of resonances. *Helv. Phys. Acta* **8** (1995) 531–538.
[21] K. Knopp, *Theory of functions*, Part II. Dover, New York (1947).
[22] P. Kravanja and M. Van Barel, *Computing the zeros of analytic functions. Lect. Notes Math.* **1727**, Springer (2000).
[23] N. Kuznetsov, V. Maz'ya and B. Vainberg, *Linear Water Waves, a Mathematical Approach*. Cambridge (2002).
[24] C. Labreuche, *Problèmes inverses en diffraction d'ondes basés sur la notion de résonances*. Ph.D. thesis, University of Paris IX, France (1997).
[25] P.D. Lax and R.S. Phillips, Decaying modes for the wave equation in the exterior of an obstacle. *Comm. Pure Appl. Math.* **22** (1969) 737–787.
[26] M. Lenoir, M. Vullierme-Ledard and C. Hazard, Variational formulations for the determination of resonant states in scattering problems. *SIAM J. Math. Anal.* **23** (1992) 579–608.
[27] T.-Y. Li, On locating all zeros of an analytic function within a bounded domain by a revised Delvess/Lyness method. *SIAM J. Numer. Anal.* **20** (1983).
[28] F. Loret, *Time-harmonic or resonant states decomposition for the simulation of the time-dependent solution of a sea-keeping problem.* Ph.D. thesis, Centrale Paris school, France (2004).
[29] G. Majda, W. Strauss and M. Wei, Numerical computation of the scattering frequencies for acoustic wave equations. *Comput. Phys.* **75** (1988) 345–358.
[30] S.J. Maskell and F. Ursell, The transient motion of a floating body. *J. Fluid Mech* **44** (1970) 303–313.
[31] C. Maury and P.J.T. Filippi, Transient acoustic diffraction and radiation by an axisymmetrical elastic shell: a new statement of the basic equations and a numerical method based on polynomial approximations. *J. Sound Vibration* **241** (2001) 459–483.
[32] M.H. Meylan, Spectral solution of time dependent shallow water hydroelasticity. *J. Fluid Mech.* **454** (2002) 387–402.
[33] L.W. Pearson, D.R. Wilton and R. Mittra, Some implications of the Laplace transform inversion on SEM coupling coefficients in the time domain, in *Electromagnetics*, Hemisphere Publisher, *Washington DC* **2** (1982) 181–200.
[34] O. Poisson, Étude numérique des pôles de résonance associés à la diffraction d'ondes acoustiques et élastiques par un obstacle en dimension 2. *RAIRO Modèle. Anal. Numér.* **29** (1995) 819–855.
[35] R.J. Prony, L'École Polytechnique (Paris), 1, *cahier 2*, 24 (1795).
[36] T.K. Sarkar, S. Park, J. Koh and S. Rao, Application of the matrix pencil method for estimating the SEM (Singularity Expansion Method) poles of source-free transient responses from multiple look directions. *IEEE Trans. Antennas Propagation* **48** (2000) 612–618.
[37] R.H. Schafer and R.G. Kouyoumjian, Transient currents on a cylinder illuminated by an impulsive plane wave. *IEEE Trans. Antennas Propagation* **ap-23** (1975) 627–638.
[38] S. Steinberg, Meromorphic families of compact operators. *Arch. Rational Mech. Anal.* **31** (1968) 372–380.
[39] S.H. Tang and M. Zworski, Resonance expansions of scattered waves. *Comm. Pure Appl. Math.* **53** (2000) 1305–1334.
[40] A.G. Tijhuis and R.M. van der Weiden, SEM approach to transient scattering by a lossy, radially inhomogeneous dielectric circular cylinder. *Wave Motion* **8** (1986) 43–63.
[41] H. Überall and G.C. Gaunard, The physical content of the singularity expansion method. *Appl. Plys. Lett.* **39** (1981) 362–364.
[42] B.R. Vainberg, *Asymptotic methods in equations of mathematical physics*. Gordon and Breach Science Publishers (1989).
[43] J.V. Wehausen and E.V. Laitone, Surface waves, in *Hanbuch der Physik* **IX**, Springer-Verlag, Berlin (1960).